

## Long-Range Crossover and "Nonuniversal" Exponents in Micellar Solutions

Michael E. Fisher

Baker Laboratory, Cornell University, Ithaca, New York 14853

(Received 14 July 1986)

Observations of apparently nonuniversal exponents at the lower consolute points of micellar solutions of *n*-dodecyl-octaoxyethylene glycol monoether in H<sub>2</sub>O, D<sub>2</sub>O, etc., are analyzed by use of crossover scaling-theory and Ising-model results. The data quantitatively sustain a picture of stable micelles of radius *R* undergoing ordinary criticality with crossover to Ising behavior delayed by an increasing range of interaction measured by  $\xi_0$ , the observed correlation-length amplitude: The crossover points,  $t_x \equiv (T_c - T_x)/T_c \sim (R/\xi_0)^6$ , vary by a factor  $\geq 10^2$  correlating with the changes seen in  $\gamma_{\text{eff}}$  and  $\nu_{\text{eff}}$ .

PACS numbers: 64.70.Ja, 05.70.Jk, 64.60.Cn, 82.70.-y

Dilute aqueous solutions of the nonionic amphiphilic molecules *n*-alkyl-polyoxyethylene glycol monoethers, i.e.,  $\text{CH}_3(\text{CH}_2)_{i-1}\text{O}(\text{CH}_2\text{OCH}_2)_j\text{H}$ , which formula will be labeled  $C_iE_j$ , exhibit the formation of micelles of well-defined size in the temperature and concentration range  $T = 10$  to  $40^\circ\text{C}$ ,  $c = 1$  to  $20$  wt.%. On raising the temperature, one finds a lower consolute point  $T_c$  above which a solution of critical concentration  $c_c$  separates into a micelle-rich and a micelle-poor phase. For  $C_6E_3$  in H<sub>2</sub>O, one has  $T_c \approx 41^\circ\text{C}$  and  $c_c \approx 13$  wt.%; however, for  $C_{12}E_8$  the critical concentration is only 3% while  $T_c \approx 74^\circ\text{C}$ .

The critical points for  $C_iE_j$  with  $i \leq 6$  and  $j \leq 3$  seem to belong to the Ising universality class, as found for ordinary binary fluid mixtures. Thus, the isothermal osmotic compressibility  $\chi \equiv (\partial c / \partial \Pi)_{T,p}$  and the correlation length  $\xi(T)$  can be well represented, for  $c = c_c$  and small  $t \equiv (T_c - T)/T_c$ , by

$$\chi(T) \approx C/t^\nu, \quad \xi(T) \approx \xi_0/t^\nu, \quad (1)$$

with exponents  $\nu \approx \nu_f \approx 0.63$  and  $\gamma \approx \gamma_f \approx 1.24$ . On the other hand, recent measurements spanning  $t \leq 10^{-4}$ – $10^{-2}$  by Degiorgio and co-workers<sup>1,2</sup> on  $C_{12}E_8$  in H<sub>2</sub>O yield  $\gamma = 0.88 \pm 0.03$  and  $\nu = 0.43 \pm 0.03$ . These exponent values are even lower than the classical (van der Waals or mean field) values,  $\gamma_0 = 1$  and  $\nu_0 = \frac{1}{2}$ . Furthermore, the critical behavior proves surprisingly sensitive to changes in the solvent: Adding salts, such as CsI, to make  $0.1 M$  solutions increases  $\gamma$  by  $0.13$ – $0.18$ . More strikingly, replacement of pure H<sub>2</sub>O by pure D<sub>2</sub>O results, at  $t \approx 10^{-4}$ , in a fivefold increase in  $\chi$ , and gives<sup>2</sup>  $\gamma = 1.20 \pm 0.03$ ,  $\nu = 0.59 \pm 0.03$ ; a 50:50 mixture yields intermediate values. (For  $t \geq 10^{-2}$ , by contrast, the changes in  $\chi$  amount to no more than  $\pm 5\%$ .)

Two types of questions arise: (a) How can the apparently "nonuniversal" critical exponents be understood in terms of changing effective interactions? Is a new type of critical behavior involved? (b) What microscopic mechanism in the solution modulates the effective interactions? How does this depend on deuteration, on the presence of salts, on the magnitude of

*i* and *j*? In this note, I argue, in answer to (a), that *no* intrinsically new critical behavior is entailed<sup>3</sup>: Specifically, I demonstrate that the detailed data are consistent with a *crossover* from classical to Ising behavior controlled by a *reduced range*  $\Lambda$  describing the interactions between micelles regarded as units.<sup>4</sup> Furthermore,  $\Lambda$  can be determined from the observations. Questions of type (b) are not addressed.<sup>5</sup>

Consider, first, the length scales. If micelles are the basic interacting units,<sup>4</sup> their radius *R*, as determined well outside the critical region,<sup>1</sup> sets the microscopic scale corresponding to *a*, the lattice spacing in discrete models or the reciprocal momentum cutoff in continuum field theories.

To test the hypothesis that the micelles act as units even through the critical region, we compare the "susceptibility"  $\chi$  with the correlation length. If  $\nu_0$  is the molecular volume, the mean number *N* ( $\gg 1$ ) of molecules in a micelle varies as  $R^d/\nu_0$  in *d* dimensions, while the density *n* of micelles varies as  $\nu_0/R^d$ . Since  $\chi$  is a fluctuation density, it is proportional to  $nN^2$ . Next note that,<sup>6</sup> quite generally,  $\chi$  should vary as  $(\xi/a)^{2-\eta}$  with  $\eta \leq 0.04$  for  $d \geq 3$ . This implies the exponent relation  $\gamma = (2-\eta)\nu$  which, to within the available precision, is well verified by all the data<sup>1,2</sup> for  $C_{12}E_8$ , on which we focus. If  $M_0$  is the molecular weight and *c* is the mass density, we thus expect

$$\chi \approx A \frac{M_0}{k_B T} n N^2 \left( \frac{\xi}{a} \right)^{2-\eta} \approx \frac{A' M_0}{\nu_0 k_B T} R^{d-2+\eta} \xi^{2-\eta}, \quad (2)$$

where *A* and *A'* are numerical constants.

It follows from (2), with the approximation  $\eta = 0$ , that the ratio  $\chi/R\xi^2$  should remain constant in the critical region as one varies the solvent, (*i, j*) being fixed. Testing this on the data<sup>2</sup> for  $C_{12}E_8$  in H<sub>2</sub>O, D<sub>2</sub>O, and a 50:50 mixture yields the values shown in rows (i)–(iii) of Table I. The constancy of the ratio, at about 4.4, is remarkable in view of the variations in  $\gamma$  (from 1.20 to 0.88). The data of Ref. 1 span a smaller range of *t* and are less precise. However, if  $\chi/R\xi^2$  is estimated by  $C/R\xi_0^2$  [in accord with (1), but at a cost in accuracy] the values listed in rows (iv)–(viii)<sup>1</sup> of

TABLE I. Data for  $C_{12}E_8$  (see text) in various solvents.<sup>a</sup> The uncertainties in fitting the exponent  $\gamma$  are  $\pm 0.03$ ;  $t_-$  and  $t_+$  specify the fitting range. Uncertainties refer to the last decimal place.

Solvent <sup>a</sup>	$R$ ( $\text{\AA}$ ) <sup>b</sup>	$[\chi/R\xi^2]^c$	$\gamma$	$\Lambda = 4\xi_0/R$	$-\log t \pm$
i $D_2O$	32	4.3 ( $\pm 3$ )	1.20	1.13 ( $\pm 26$ )	2.0/4.0
ii 50:50	33.5 <sup>d</sup>	4.3 <sub>5</sub> ( $\pm 4$ )	1.03	1.79 ( $\pm 30$ )	2.0/4.0
iii $H_2O$	35	4.4 ( $\pm 4$ )	0.88	2.63 ( $\pm 43$ )	2.0/4.2
iv $D_2O$	34	6.0 ( $\pm 28$ )	1.18	1.19 ( $\pm 31$ )	1.6/3.2
v aq <sub>v</sub>	33	10 ( $\pm 4.5$ )	1.06	1.37 ( $\pm 33$ )	1.6/3.2
vi aq <sub>vi</sub>	35	8.6 ( $\pm 41$ )	1.03	1.14 ( $\pm 30$ )	1.6/3.2
vii aq <sub>vii</sub>	35	4.4 ( $\pm 20$ )	1.01	1.40 ( $\pm 36$ )	1.6/3.2
viii $H_2O$	34	4.6 ( $\pm 15$ )	0.92	2.26 ( $\pm 52$ )	1.6/3.2

<sup>a</sup>See Ref. 2 for (i)–(iii); Ref. 1 for (iv)–(viii); the 0.1  $M$  aqueous solutions contain: (v) CsI, (vi)  $(CH_3)_4NH$ , and (vii) CsCl.

<sup>b</sup>Uncertainties in  $R$  ( $\equiv R_H$ , see Ref. 2) are  $\pm 2 \text{\AA}$ .

<sup>c</sup>In units of  $10^{13} \text{ cm}^{-5} \text{ s}^2$ . The absolute calibration factor found for  $H_2O$ , (iii), has been used also for (i) and (ii).

<sup>d</sup>Interpolated between (i) and (iii).

the table are found: These are consistent with a constant value around 4.5.

To understand the variations in  $\gamma$ , consider the *interaction range*  $b$ , which is best defined theoretically via the second moment of the attractive part of the potential. Following Ornstein and Zernike,<sup>6</sup> one knows that  $b$  is intimately linked to the scale of propagation of correlations, and may thence be identified with the amplitude  $\xi_0$  in (1). Accordingly, we define the reduced interaction range by  $\Lambda = 4\xi_0/R \propto b/a$ , where no special significance attaches to the factor 4. Now the various solutions in Table I are listed (separately for Refs. 1 and 2, since very different ranges of  $t$  are spanned) in order of decreasing magnitude of the fitted exponent  $\gamma$ . Note that, except for solution (vi), the order is *also* one of *increasing*  $\Lambda$ . The data are thus consistent with the idea, based on the Ginsburg criterion and the long-range, Kac–van der Waals limit, that increasing  $\Lambda$  induces a crossover from nonclassical to classical critical behavior and hence leads to an apparent decrease in  $\gamma$ .

The objection might be raised that such a crossover could not yield values such as  $\gamma \approx 0.88$ , which lie outside the range  $\gamma_1 \approx 1.24$  to  $\gamma_0 = 1$ . But this objection cannot be sustained in the absence of reliable calculations of the *form* of the crossover. To describe that, the effective exponent function<sup>7</sup>  $\gamma_{\text{eff}}(t) = d \ln \chi / d \ln t$  is useful. This approximates the value of  $\gamma$  centered at  $\log t$  given by log-log fits over a decade or two. Now,  $\gamma_{\text{eff}}$  should approach  $\gamma_1$  as  $t \rightarrow 0$  and  $\gamma_0$  for “large”  $t$ ; however, the approaches *need not* be monotonic. Thus, nearest-neighbor  $d=3$  Ising models exhibit an approach to  $\gamma$  from *above* with  $\gamma_{\text{eff}} \approx 1.250$  for  $t \approx 10^{-3}$ , but a decrease towards  $\gamma_1 \approx 1.239$  for smaller  $t$ .<sup>8</sup> Furthermore, explicit renormalization-group calculations<sup>9</sup> to order  $\epsilon = 4 - d$  for crossover from Ising to  $XY$  or Heisenberg, etc., reveal complex behavior with

“overswings” and “underswings” which can even *exceed* the total asymptotic change in  $\gamma$ . For  $C_{12}E_8$ , the observed overswing<sup>2</sup> is about  $1.00 - 0.88 = 0.12$  which is only 50% of  $\Delta\gamma = \gamma_1 - \gamma_0$ .

The nature of the crossover should be described by standard scaling theory.<sup>6</sup> If  $g$  denotes the leading irrelevant variable, associated with the energy amplitude  $U_4$  of the  $s^4$  term in an equivalent spin Hamiltonian, the crossover from classical behavior is given by<sup>6</sup>

$$\chi(T, g) \approx t^{-1} X(g/t^\phi), \quad (3)$$

with  $\phi = \frac{1}{2}\epsilon$  for  $\epsilon \equiv 4 - d > 0$ . The exponent  $\phi$  is exact and, for  $a/b$  not too large,<sup>9,10</sup> one has  $g \propto U_4(a/b)^d$ . Differentiating (3) and rearranging yields

$$\gamma_{\text{eff}}(t) = 1 + \Delta\gamma E(\ln t - \ln t_\times), \quad (4)$$

in which  $\Delta\gamma = \gamma_1 - \gamma_0 \approx 0.24$  while the *crossover temperature* varies as

$$t_\times \propto (U_4/k_B T)^{2/\epsilon} (a/b)^{2/\epsilon} \approx B \Lambda^{-2d/\epsilon}. \quad (5)$$

This last result is essentially that given by the Ginsburg criterion for the validity of classical theory. In treating  $B$  as a constant, we suppose that the variation of  $U_4/k_B T$  is not significant compared to that produced by  $\Lambda$  which, for  $d=3$ , carries an exponent of  $-6$ . In a convenient normalization, the exponent crossover function must, as usual, satisfy<sup>6,9</sup>

$$E(\ln y) = 1 \pm y^\theta + \dots \text{ as } y \rightarrow 0, \\ \approx E_\infty / y^{\epsilon/2} \text{ as } y \rightarrow \infty, \quad (6)$$

where  $\theta = \frac{1}{2}\epsilon + O(\epsilon^2)$  ( $\approx 0.5$ ,  $d=3$ )<sup>8</sup> is the leading correction-to-scaling exponent.

Now, to order  $\epsilon$  one actually finds<sup>9</sup>

$$E(\ln y) = 1/(1 + y^{\epsilon/2}). \quad (7)$$

The corresponding  $\gamma_{\text{eff}}$  for  $d=3$  is represented by the solid curve in Fig. 1. (The convenient assignment  $t_x = 10^{-3.5}$  has been used.) The full crossover is spread over four or five decades, the gradient  $\Gamma = -\partial\gamma_{\text{eff}}/\partial\log t$  achieving a maximum of 0.069 per decade. However, over the interval  $\gamma_{\text{eff}}=1.21-1.13$  the gradient is only  $\Gamma=0.056$ . This may be compared with results for the "equivalent neighbor" fcc Ising model in which each spin has *equal* couplings,  $J$  to all spins in its first  $k$  neighboring shells.<sup>11</sup> Ratio analysis of the series for  $\chi$  to orders from  $(J/k_B T)^6$  to  $(J/k_B T)^8$  gives a  $\gamma_{\text{eff}}$  for  $t \approx 10^{-2.5}$  of  $1.252(\pm 0.003)$  for  $k=1$  (nearest neighbor),  $1.226-1.198$  for  $k=2$  (next-nearest neighbor) but only  $1.113-1.148$  for  $k=3$ .<sup>12</sup> On the other hand, by geometry one finds  $\Lambda_k \equiv b/a = 1, (\frac{4}{3})^{1/2}$  and  $(\frac{16}{7})^{1/2}$  for  $k=1, 2, 3$ . Via (5), one obtains a gradient  $\Gamma = 0.116 \pm 0.011$  per decade, which is evidently *twice* as large as the  $O(\epsilon)$  prediction for the same  $\gamma$  interval.

Clearly then, computations to higher order in  $\epsilon$  would be desirable but, to our knowledge, none are available. Such calculations should also involve the coefficients  $U_5$  and  $U_6$  of the equivalent  $s^5$  and  $s^6$  terms which may, indeed, play a role in producing nonmonotonicity with  $\gamma_{\text{eff}} < 1$ .<sup>13</sup> In the absence of further theoretical results, the approximant

$$E(\ln\gamma) \approx (1 + py^{\epsilon/2})/[1 + (p+1)y^{\epsilon/2} + qy^\epsilon]$$

may be used: It satisfies (6) and reduces to (7) when  $p=q=0$ . For  $p$  and  $q$  of order  $\epsilon$ , it should thus provide reasonable results since even at  $d=3$  we have  $\theta \approx \frac{1}{2}$ . The dot-dash curve in Fig. 1 (for  $\epsilon=1$ ) corresponds to  $p=-1.36, q=0.74$ , and the assignment  $t_x = 10^{-3.1}$ ; these quite reasonable parameters provide a very plausible fit to the experimental data which have been plotted according to the following procedure.

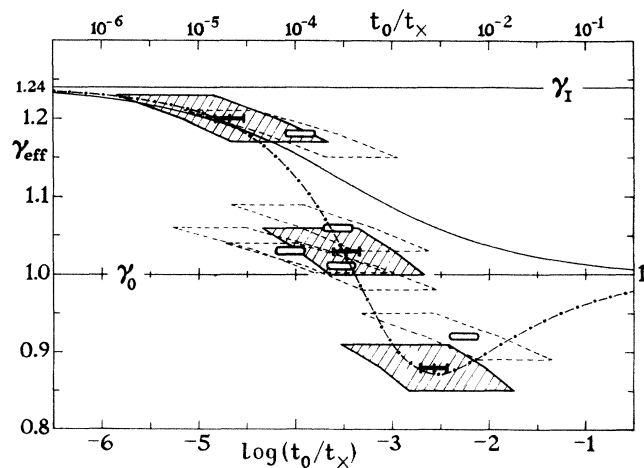


FIG. 1. The effective exponent  $\gamma_{\text{eff}}$  vs reduced fitting and crossover temperatures,  $t_0$  and  $t_x$ : see Table I and text.

First I use the data for  $\Lambda$  in Table I to compute  $t_x$  according to (5), in which I choose for  $B$  the arbitrary but *fixed* value  $10^{-5}$ . (Changing  $B$  merely translates the plot along the  $\log t$  axis.) Given the range over which  $\gamma$  is fitted, say,  $t_-$  to  $t_+$  as listed in the table, I take the geometric mean  $t_0 = (t_- t_+)^{1/2}$  as the mid-range value of  $t$ . Then to check (4) I plot the central estimate for  $\gamma$  vs  $\log(t_0/t_x)$ . Solid symbols are used for the most precise and extensive data, namely, for solutions (i)-(iii)<sup>12</sup>; open symbols denote the older data, (iv)-(viii).<sup>1</sup> The width of the symbols specifies the uncertainty arising in  $\Lambda$  from the measurement<sup>1</sup> of the micelle radius,  $R$ . The heights of the surrounding slanted boxes represent the uncertainties in  $\gamma$ . The widths of the boxes correspond to *half* the fitting range ( $\log t_-, \log t_+$ ).

The sides of the boxes in Fig. 1 have been slanted in order to represent a correlation between the deviations in the  $\xi_0$  and  $\gamma$  estimates. To understand this, note first that uncertainties in  $\xi_0$  enter into  $t_x$  via  $\Lambda$ . Second, recall that  $\eta \approx 0$ , so that we expect, and find,  $\gamma \approx 2\nu$ . Thus, a low estimate for  $\gamma$  should correspond to a low estimate for  $\nu$ . When one examines the crossover in  $\nu_{\text{eff}}$ , for which all the parallel considerations apply (see Fig. 2), this step is not needed. Finally, because all the data fitted lie below  $t = 10^{-1.6}$ , a *low* estimated slope on a log-log plot for  $\xi(T)$  entails a *high* estimate for the amplitude  $\xi_0$  and, hence, a *less negative* value for  $\log(t_0/t_x)$ . Thus boxes slanting with a slope  $\delta\gamma_{\text{eff}}/\delta\log(\xi_0)^6$  give a more informative view of the data than would vertically sided boxes<sup>14</sup>; likewise for  $2\nu_{\text{eff}}$  in Fig. 2. However, the reader is free to imagine rectangles if preferred.

The plotted data in Figs. 1 and 2 exhibit two crucial features: (a) they specify a rather well-defined crossover scaling function for the effective exponents,  $\gamma_{\text{eff}}$  and  $\nu_{\text{eff}}$ ; and (b) the scale of the crossover corresponds

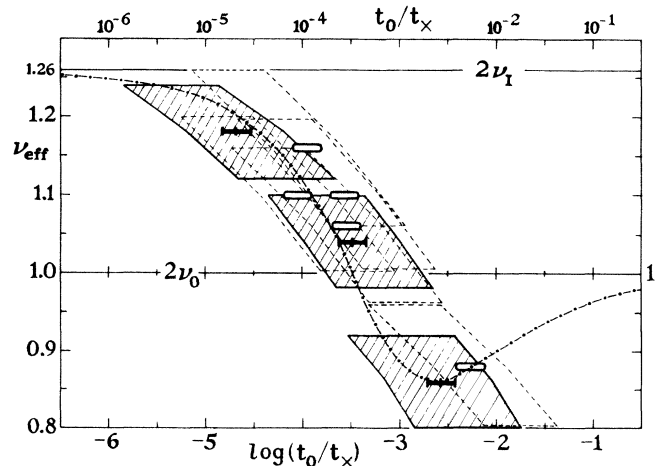


FIG. 2. Variation of the effective exponent  $2\nu_{\text{eff}}$  as in Fig. 1 with the same fitting parameters  $p$  and  $q$  but with use of  $t_x = 10^{-3.2}$ .

closely to that expected theoretically (which is mainly determined by  $\theta \simeq \phi = \frac{1}{2}$ ). More precisely, for  $\gamma_{\text{eff}}$  in the interval (1.05, 1.20) the gradient is about  $\Gamma = 0.14 \pm 0.03$ , which is only 20% larger than found for the fcc Ising model in the range (1.13, 1.21). Indeed the gradient of the dot-dashed, fitted curve in the latter interval is *lower* than for the Ising data! We conclude that the data for the whole range of  $C_{12}E_8$  systems is consistent with a crossover from classical to Ising critical behavior controlled by a varying range of effective micelle-micelle interactions which is measured by the amplitude  $\xi_0$  of the overall correlation length. There is no need to invoke some new or exotic type of criticality.<sup>3</sup>

Naturally some questions remain. On the theoretical side, concrete calculations yielding  $\gamma_{\text{eff}} < 1$  would be valuable. It might be possible to perform appropriate renormalization-group calculations to higher order in  $\epsilon$ . Ising-model series expansions might also be feasible for models with longer-range interactions. Of course, a basic microscopic issue is to gain some understanding of how the range  $\Lambda \sim \xi_0$  is so readily varied.

On the experimental side, more precise measurements of  $c_c$  and  $R$  could shed further light on the picture of micelles as fixed units.<sup>15</sup> It may also be possible to extend the domain of the range parameter  $\Lambda$ . Perhaps adding salts to a  $D_2O$  solution will reduce  $\Lambda$  and yield  $\gamma_{\text{eff}}$  closer (or even exceeding) 1.24. Conversely, if  $\Lambda$  could be increased further, one should expect to see  $\gamma_{\text{eff}}$  going through a minimum and then rising back to  $\gamma_0 = 1$ . Insofar as the dot-dash fit in Fig. 1 is realistic, an increase in  $\Lambda$  by a factor of 2 beyond that for  $C_{12}E_8$  in  $H_2O$  should yield  $\gamma \simeq 0.96$ . Solutions of  $C_{14}E_8$ ,  $C_{14}E_{10}$ , etc., might enter this region and provide a stronger test of the interpretation advanced here.

I am indebted to Vittorio Degiorgio for informative discussions and for providing me with the experimental data. Conversations with Ben Widom, Stanislas Leibler, and Raymond E. Goldstein are much appreciated. The support of the National Science Foundation (Grant No. DMR-81-17011) is gratefully acknowledged.

<sup>1</sup>V. Degiorgio, R. Piazza, M. Corti, and C. Minero, *J. Chem. Phys.* **82**, 1025 (1985).

<sup>2</sup>M. Corti and V. Degiorgio, *Phys. Rev. Lett.* **55**, 2005 (1985), and private communication, in particular regarding the amplitudes  $C$ , and the micelle radii in  $H_2O$  and  $D_2O$ .

<sup>3</sup>Y. Shnidman, *Phys. Rev. Lett.* **56**, 201 (1986), has proposed a new sort of criticality controlled by a marginal variable. However, his renormalization-group arguments are untenable. See, R. G. Caflish, M. Kaufman, and J. R. Banavar, *Phys. Rev. Lett.* **56**, 2545 (1986); L. Reatto, to be published; A. Crisanti and L. Peliti, to be published.

<sup>4</sup>For the validity of this picture away from criticality, see J. B. Hayter and M. Zulauf, *Colloid Polym. Sci.* **260**, 1023 (1982); L. Reatto and M. Tau, *Chem. Phys. Lett.* **108**, 292 (1982).

<sup>5</sup>L. Reatto and M. Tau, private communication, have suggested that three-body micellar forces play a role.

<sup>6</sup>See, e.g., M. E. Fisher, in *Critical Phenomena*, edited by F. J. W. Hahne, Lecture Notes in Physics Vol. 186 (Springer-Verlag, Berlin, 1983).

<sup>7</sup>J. S. Kouvel and M. E. Fisher, *Phys. Rev.* **136**, A1626 (1964).

<sup>8</sup>See, e.g., J.-H. Chen, M. E. Fisher, and B. G. Nickel, *Phys. Rev. Lett.* **48**, 630 (1982). Note  $b^2(y)$  should be  $\frac{1}{2}(1-y)$ .

<sup>9</sup>See, e.g., P. Seglar and M. E. Fisher, *J. Phys. C* **13**, 6613 (1980), in which Eq. (3.1) for  $\bar{u}$  lacks a factor  $a'^\epsilon$ , where  $a' = a^2/\pi R_0$ ; also,  $a'^{-\epsilon}$  should appear in (3.2),  $a$  should be replaced by  $a'$  in (3.3), etc.

<sup>10</sup>The full expression is  $g = \bar{u}(b/a)^\epsilon/(1-\bar{u})$  with  $\bar{u} \equiv u/u^* \propto (U_4 T/k_B T_0^2)(a/b)^4$ , where  $T_0 \simeq T_c$  is the mean-field critical temperature. See further Refs. 6 and 9.

<sup>11</sup>C. Domb and N. W. Dalton, *Proc. Phys. Soc. London* **89**, 859 (1966).

<sup>12</sup>The lower  $\gamma$  estimates for  $k=2$  and 3 follow from the last few ratios are normally plotted (Ref. 11). The upper estimates are obtained by use of "n-shifts" (of  $\frac{1}{2}$  and 1) to remove the curvature of the plots. Both procedures separately yield similar values of  $\Gamma$ .

<sup>13</sup>Reatto and Tau (Ref. 5) stress the likely importance of the  $U_5$  term.

<sup>14</sup>The uncertainties in  $2\nu$  are twice those in  $\gamma$ , so that the slopes are about half those on the plots for  $2\nu_{\text{eff}}$  (Fig. 2), for which the argument applies more directly.

<sup>15</sup>If all  $C_j E_j$  solute molecules are in micelles of statistically fixed shape and mean radius  $R$ , the critical micelle density relative to close-packed micelles should be constant, independent of the solvent at about  $\bar{n}_{0c} \simeq \frac{1}{3}$  (by the law of corresponding states). The overall critical mass density, for sufficiently large micelles, should then be proportional to  $M_0/v_0$  but should not depend on  $R$ , which changes somewhat as the solvent varies. The observed critical concentrations for  $H_2O$  and  $D_2O$ , namely (Ref. 2) 3.0 and 2.5 wt.%, respectively, differ in a direction consistent with this hypothesis although the precision is too low for a proper test.